UNDERSTANDING MOLYBDENUM FILMS - CHALLENGES FOR MOLYBDENUM POST CMP CLEANING FORMULATIONS

Daniela White[1*], Atanu Das[1], YoungMin Kim[2], Chun-I Lee[3], Roger Luo[3], Maryam Farmand[1] and Michael White[1]

[1]Entegris Danbury USA, daniela.white@entegris.com,
[2]Entegris KTC (Korea Technology Center)
[3]Entegris Taiwan Technology Center (TTC)

INTRODUCTION

The performance of large-scale integrated circuits and memory devices has recently become limited by their interconnects due to strongly increasing line via resistances and deteriorating reliability [1]. Chemical Mechanical Planarization (CMP) processes are currently widely used to planarize and remove excess dielectric (ILD) between conducting metal layers, as well as in damascene processes involving metal interconnect lines (copper or tungsten) or plugs (tungsten). Tungsten is a key material for connecting logic and memory devices, thanks to its excellent planarization, filling, mechanical (low mismatch of coefficient of thermal expansion with silicon) and electromigration properties (high melting temperature). As technology nodes continue scaling down, a tungsten alternative as diffusion barrier/plug might be required. Molybdenum barrier lines or plugs could be excellent tungsten replacements, due to the high melting point, elevated thermal stability, and good corrosion resistance. In addition, for 3D-NAND memory applications, Mo surfaces could offer a much smoother alternative to rougher W surfaces.

Chemical Mechanical Planarization, CMP, followed by post-CMP cleaning of Mo thin films leaves passivating Mo oxide layers (MoO_3, MoO_{3-x}, MoO_2) on the planarized/cleaned Mo surfaces. The impact of the slurry abrasive particles (type: TiO_2 vs. SiO_2, size, charge), pH and chemical additives/passivation reagents on the Mo cleaning performance and surface chemistry is discussed. Numerous surface characterization techniques such as: SEM, XPS, FTIR-Raman, particle size/charge etc., were used to understand the composition of the polishing by-products, as well as the Mo/Mo oxide surface chemistries, before and after the post-CMP cleaning processes. XPS and Raman spectroscopies show that post-CMP cleaned Mo surfaces are passivated with Mo oxides (admixtures of Mo^{6+}, Mo^{5+}, Mo^{4+}) with the highest Mo^{6+} atom % being measured on the Mo films polished with TiO_2-based abrasive slurries.

BACKGROUND

Alternatives to Cu or W metallization have been recently extended to several new metals such as Co, Ru and Mo [2 – 4]. The ideal interconnect metal should have low bulk resistivity to grain boundary or interface scattering. Recent studies on Mo thin film electrical properties indicate that Mo can be used as an alternative to Cu in logic circuit interconnects and W in 3D NAND memory applications, providing that the Mo metallic interface is totally free of oxides and other contaminants [1]. Similar to W surface chemistry, the Mo surface is passivated by a native mixed valence oxide layer up to 30Å in thickness. Park et al. showed XPS measurements on Mo films etched in H_2O_2 solutions @ pH = 2-10, indicating the formation of mixed valence oxides, with sub-stoichiometric Mo^{5+} oxides dominating the surface [5]. In addition, an oxidation-dissolution polishing mechanism was proposed with silica abrasive-based slurries at low and high pH (pH = 2-10). In acidic conditions, Mo removal was suggested to be mainly driven by mechanical abrasion, while at high pH, Mo and Mo oxide dissolution seemed to be the main removal mechanism. He et al. studied low pH Mo CMP with silica-based abrasive slurries and KIO_3 as oxidizer [6]. XPS, in-situ OCP and nanoindentation measurements showed Mo passivation with a mixture of soft Mo^{6+}/Mo^{5+} mixed oxides, easily removed by the silica-based abrasive or simply, undergoing dissolution to molybdate anions at pHs > 6. None of the publications mentioned above support the suggested polishing mechanism with a better understanding or characterization of the actual slurry waste, captured in real time during the CMP experiments. Our mechanistic experiments involving slurry waste characterization cover two different types of slurry abrasives, TiO_2 and SiO_2. There are no literature reports so far on Mo film CMP with TiO_2-based slurries. TiO_2-based slurry abrasives in the presence of H_2O_2 as oxidizer were previously developed by us for bulk Ru CMP, with RR > 1000 Å/min [7], [8]. Strong oxidizing species generated by H_2O_2

ENTEGRIS PROPRIETARY AND CONFIDENTIAL – INTERNAL

adsorption/decomposition on the TiO_2 nanoparticles surface to superoxide anion-radicals are responsible for the high metal removal rates (e.g. Ru, Mo). Reversible formation of both superoxide radical anions on the particle/catalyst surface and reduced Ti^{3+} cations on the wafer surface simultaneously occur with the metal oxidation and TiO_2 surface regeneration towards chemisorption of more oxidizer, generating of new surface-active radicals. Other acute and perpetual requirements pertaining to both W and Mo films are delivering post-CMP defect-free, clean surfaces, with low Mo/W static etch rates (< 0.5 Å/min) and other Mt^{n+} residue < 10^{10} atoms/cm^2. It is of utter importance to understand the surface chemistry, Mo oxidation states and the type of surface Mo oxides formed during CMP vs. slurry abrasive particles vs. pH, and in the next step, the chemical transformations occurring during post-CMP cleaning with complex formulations at different pHs.

EXPERIMENTAL

TiO_2 and SiO_2 based polishing slurries are described in Table 1. The post-CMP cleaning formulations are based on: Mo corrosion inhibitor, silica particles dispersants, organic residue dissolution additives, MoOx and molybdates dispersants, metal cations chelating ligands, pH adjustors. The pH was adjusted to cover a large range, 2-13.

200 mm Mo, PETEOS and Si_3N_4 blanket wafers (each one 5000 Å film thickness) deposited via PECVD on prime silicon substrate were purchased from Advantiv Technologies Inc. In preparation for the polishing/cleaning experiments, each blanket wafer was cut into 2×1 cm^2 rectangular coupons, rinsed with isopropyl alcohol for 30 seconds, rinsed with deionized water for 1 minute and dried under nitrogen.

All three films were polished on an IC 1000-XY/SUBA pad, using a Buehler AutoMet 300 bench-top polisher at 3.0 psi downforce. The platen/carrier speed and the slurry flow rate were 80/100 rpm and 50 mL/min, respectively. The 1 min CMP pad conditioning between each sample was performed with a diamond disc to avoid cross-contamination with the CMP byproducts. Slurry waste dispersion was captured during polishing and then filtered, dried, and characterized by XPS, Raman, FTIR and particle size/zeta potential measurements. In some cases, the slurry waste supernatant was separately dried and characterized by the FTIR.

Mo, PETEOS and Si_3N_4 etch rates were measured by ellipsometry, using a JA Woolam M-2000D Ellipsometer. Fourier transform infrared spectroscopy with attenuated total reflection (FTIR-ATR) measurements of Mo films and dried slurry waste were performed using a Thermo Scientific™ Nicolet™ iS50 FTIR Spectrometer. Analysis of the resulting spectra was performed with OMNIC software.

Raman spectroscopy measurements of Mo films and dried slurry waste were collected using a LABRAM HR microscope from Horiba and the data was analyzed using LabSpec6 software, laser wavelength of 532 nm (50 mW) and objective 10X or 50X.

SEM measurements were performed using a Hitachi SU8000 field emission SEM. This was a top-down analysis on a 26μmx26 μm surface area, utilizing a low angle detector (secondary electrons) at a voltage of 5kV and a current of 20μA.

XPS surface characterization was performed by X-ray photoelectron spectroscopy using a PHI VersaProbe II Scanning XPS Microprobe, with the Al K_α line at 1486.6 eV as the X-*ray* source, a standard acceptance angle, a 45° take-off angle, a 1000 μm x 100 μm analysis area and the C1s 284.8 eV line for charge correction.

Slurry and slurry waste particle size and zeta potential were measured using a Nicomp Particle Size Solutions Z3000 instrument and analyzed using Nicomp ZPW388 Application version 2.18.

Table 1

Slurry	Slurry abrasive	Particle size, nm	Mo passivating reagent	Mt catalyst	Oxidizer	pH
TiO_2 Slurry	TiO2 (rutile/anatase mixture)	40	1x	1x	1x	2.5
Slurry A	SiO_2 Supplier 1	60	1x	1x	0.1x	2.3
Slurry B	SiO_2 Supplier 1	60	1x	2x	1x	2.3
Slurry C	SiO_2 Supplier 2	120	2x	1x	0.1x-1x	2.3

DISCUSSION

1. Chemical-Mechanical Planarization of Mo with TiO_2-Based Slurries

Decomposition of hydrogen peroxide on solid Lewis acid oxide surfaces (zirconia, ceria, titania, alumina) at room temperature, in aqueous dispersions is, regardless of the oxide, a first order reaction and the calculated activation energy is similar for all four oxides, around 42 kJ/mol, considerably less than 210 kJ/mol needed for the homolytic cleavage of the O-O bond in H_2O_2, leading to the conclusion that the water-oxide interface is catalytically lowering the energy barrier for H_2O_2 decomposition, [9]. Previous ESR studies on the MtO_2/H_2O_2 particles (Mt = Ti, Zr, Ce) have already evidenced the presence of long-lived paramagnetic superoxide oxygen radical anions on the surface of TiO_2, following H_2O_2 catalytic decomposition.

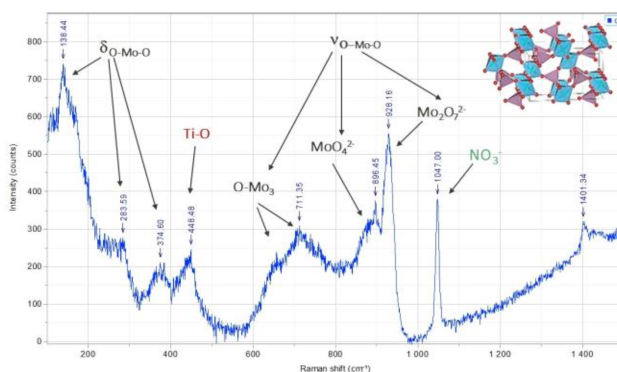

Figure 1 Raman spectrum of Ti molybdate slurry waste

Figure 1 shows the Raman spectrum of the slurry waste collected during polishing Mo films with the TiO_2/H_2O_2 slurry, at pH = 2.3. The spectral features between 900-600 cm^{-1} and 400-200 cm^{-1} are characteristic to Mo-O stretching vibrations (O-Mo_3 triply coordinated oxygen, orthorhombic structure, also MoO_4^{2-} and the dimer $Mo_2O_7^{2-}$) and bending (O-Mo-O scissoring and wagging) modes, respectively. In addition, the Ti-O stretching vibration as in titanium molybdates, occurs around 450 cm^{-1}. [10]

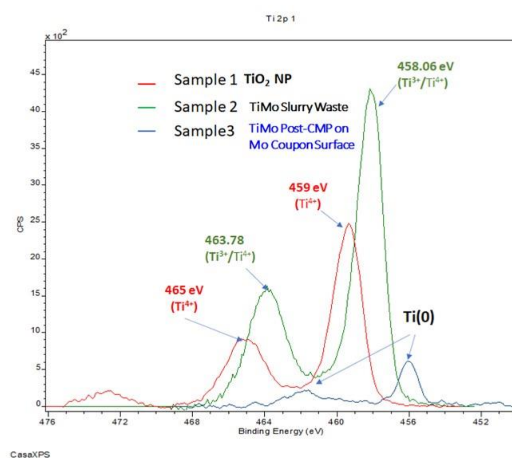

Figure 2 Ti 2p XPS deconvoluted spectra of TiO2, dry slurry waste and Mo surface contamination

Figure 2 represents an overlay of the Ti 2p XPS spectra: control TiO_2-based slurry, dried slurry waste and polished Mo film surface. There is a shift towards lower energies and hence lower oxidation states from sample 1 (TiO_2 NP) to sample 2 (slurry waste). In other words, there was an increase in the reduced Ti^{3+}

species in the slurry waste. In addition, the higher electronegativity of Mo compared to Ti, suggests a lattice shift by the substitution of Mo^{6+} for Ti^{4+} ion (slurry waste and Mo film surface), in a similar way to the Ru polishing mechanism. The presence of the reduced Ti oxidation states (3+, 0) also suggests an additional redox interaction between the two metals, Mo (0) being oxidized also by the Ti^{4+}, along with the superoxide radical anions on the TiO_2 nanoparticles surface.

TiO_2 polished Mo surface chemistry and the admixture of oxides layer will be discussed in the next section, as compared with the SiO_2-slurry abrasive, based on the Mo 3d XPS data presented in Figures 11 and 12.

2. Chemical-Mechanical Planarization of Mo with SiO_2-Based Slurries

Three silica-based slurries (Slurry A, Slurry B, Slurry C, Table 1) were prepared and used to planarize our three substrates, Mo and two dielectric films, PETEOS and Si_3N_4. In order to see a potential effect of the dielectric films polishing by-products on the Mo removal rates, the experiment was designed to polish first all three films together (one Mo coupon + one PETEOS coupon + one Si_3N_4 coupon), followed by each film or single substrate: 3 Mo coupons, 3 PETEOS coupons, 3 Si_3N_4 coupons. Also, 6 repeats of each type of set-up were run to potentially detect any run-order effect (removal rate variations, surface composition changes, etc.).

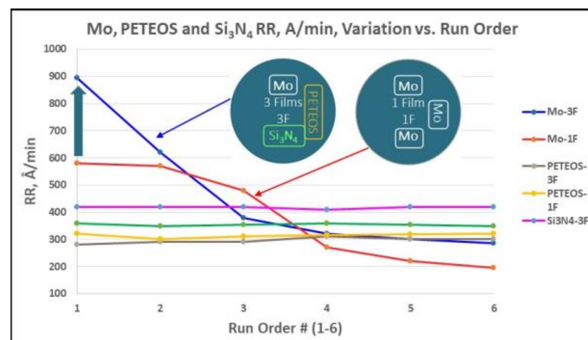

Figure 3 Mo, PETEOS and Si_3N_4 RR vs. run order

Figure 3 shows the effect of run order on the removal rates for the two set-ups (three films polished together vs. one film at a time), using Slurry B. Mo removal rates were the most affected by both run order and types of films polished together or single film. In the three films set-up, Mo removal rates were 1.5X higher than one-film set-up, for coupon/run #1, followed by a sharp decrease in rate with the increase in run order, for both set-ups. Both PETEOS and Si_3N_3 removal rates remained mostly unaffected by the run order or the set-ups (three films vs. one film).

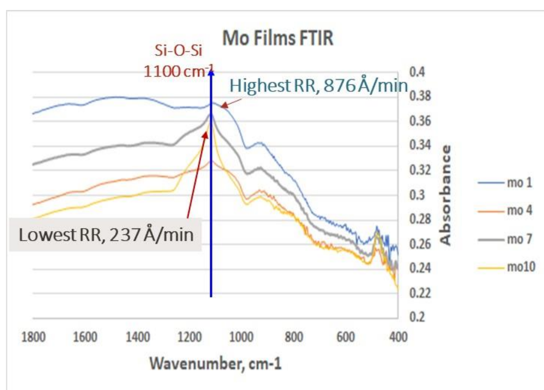

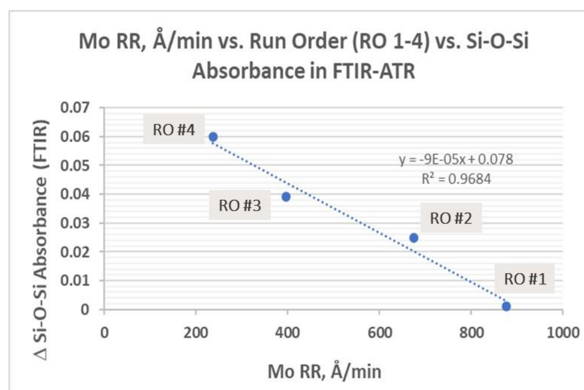

Figure 4 FTIR spectra of polished Mo films vs.

Figure 5 Correlation Mo RR, Å/min vs. run order

Figure 4 shows the overlay of the FTIR spectra of the Mo films (three films set-up) run order 1-4. The Si-O-Si very weak vibration (~ 1100 cm-1) for run #1 becomes stronger with the progression in the run order, so, finally, for the run #4 the signal is the strongest, dominating the whole spectrum. A very good correlation between the increasing of the Si-O-Si surface bond and Mo decreasing removal rates plotted as the Figure 5 confirms that a run-order driven SiO_2 layer (from both slurry abrasive and dielectrics polishing by-products) is responsible for the decrease in Mo removal rates from run #1 to run #6.

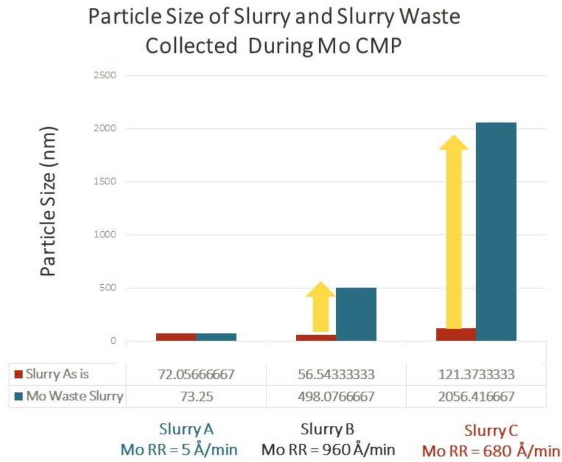

Figure 6 Particle size slurry vs. slurry waste

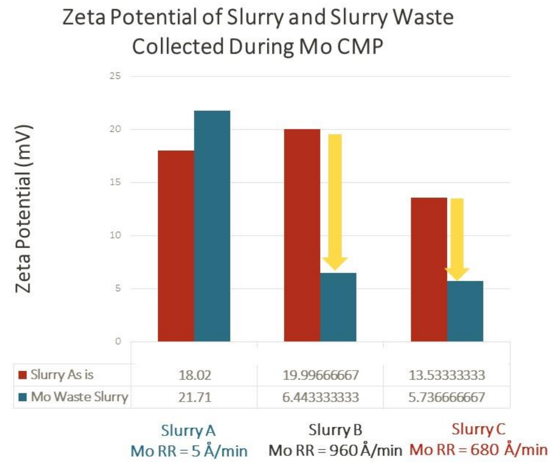

Figure 7 Variation of zeta potential in slurry/slurry waste

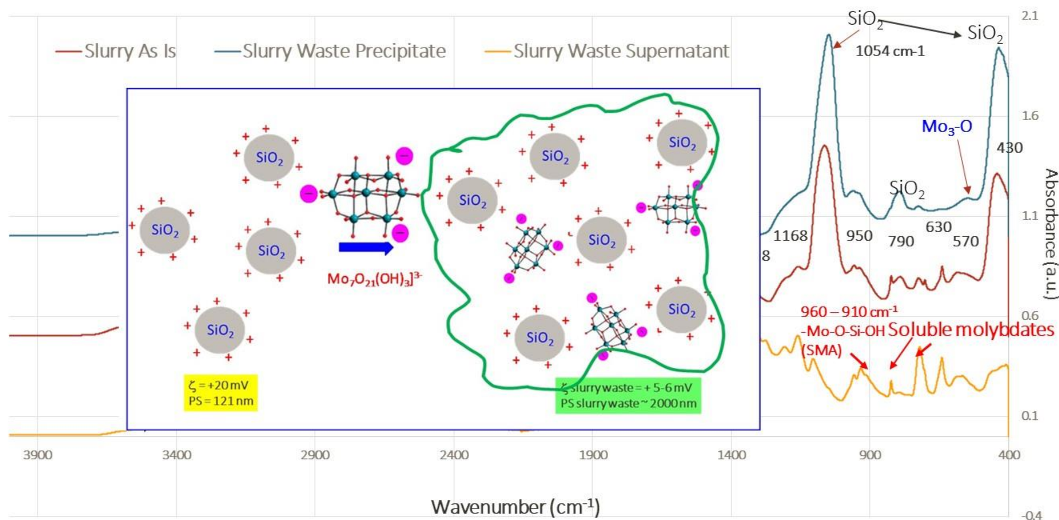

Figure 8 FTIR of control slurry, dried slurry waste and dried slurry waste supernatant

Slurry waste from all three silica-based slurries (A, B and C) were captured during Mo films polishing and characterized for particle size/zeta potential, FTIR, XPS and Raman. Figures 6 and 7 show substantial changes in both particle size and zeta potential for the slurry waste comparative to the control slurries. In all slurry waste samples, the mean particle size increases by 10-15X while the zeta potential (of the positive charged control particles) decreases by a factor of 2-3. Figure 8 overlays three FTIR spectra for the dried control slurry particles (Slurry C), dried slurry waste and dried slurry waste supernatant. Slurry waste is mainly composed by silica particles (1060 cm-1) with a minuscule shoulder around 580 cm^{-1}, which was assigned to the stretching mode of the triply-coordinated oxygen (Mo_3–O), which results from the edge-shared oxygen in common with three MoO_6 octahedra. On the other hand, the dried slurry waste supernatant shows mainly aqueous molybdate species [11-12], including silicomolybdic acid peaks between 960-910 cm^{-1}. The particle agglomeration mechanism is believed to be due the positively charged silica particles crosslinking by the most prevalent aqueous peroxo- and heptamolybdate anionic species, $Mo_7O_{21}(OH)_3^{3-}$, together with trace amounts of MoOx, vaguely detected by FTIR. Notably to report that Mo 3d XPS analysis also detected only trace amounts of Mo in the slurry waste, not possible to deconvolute, slurry waste composed > 99% atoms Si (survey spectrum).

3. Post-CMP Cleaning: pH effect of particle defectivity and surface Mo oxidation states

A post-CMP cleaning formulation based on Mo corrosion inhibitor, silica particles dispersants, organic residue dissolution additives, MoOx and molybdates dispersants, and metal cations chelating ligands had the pH adjusted to three values (2, 6 and 13), covering a wide range in the acidic and alkaline regions.
Figure 9 shows the particle defectivity areas on Mo, PETEOS and Si_3N_4 films, polished with the low pH silica-based Slurry C and cleaned with the acidic, neutral, and alkaline cleaning formulations. All three films had the minimum level of contaminants/best cleaning performance with the cleaning formulation at pH 13. Static etch rates @ 30°C for Mo, PETEOS and Si_3N_4 were all low, 0.95A/min, 0.12A/min and 0.06A/min, respectively.

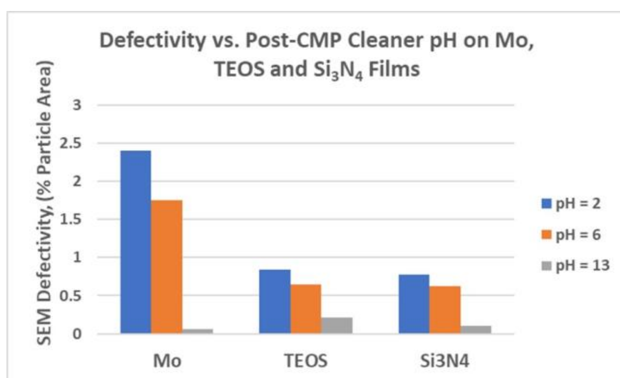

Figure 9 Particle defectivity vs. cleaner pH

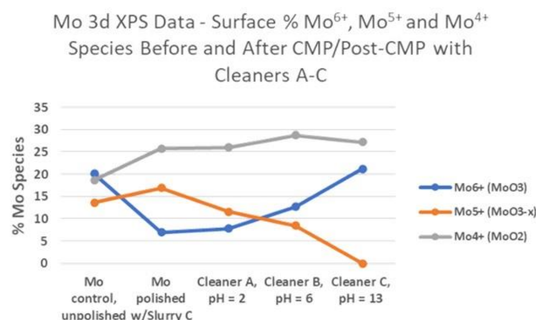

Figure 10 Mo 3d XPS Spectra vs. cleaner pH

The surfaces of the cleaned Mo coupons with the various low and high pH post-CMP cleaning formulations were further characterized by XPS spectroscopy. Figure 10 represents the surface % oxidized Mo^{n+} atoms for the three films, as compared with the control/unpolished and polished film with Slurry C. The most striking changings in the Mo oxidation states vs. the unpolished and polished controls are detected for the higher oxidation states, Mo^{5+} as in MoO_{3-x} suboxides (sharp decrease with the pH increase) and Mo^{6+} as in MoO_3, (sharp increase with the pH increase). The increase in the MoO_3 surface layer at alkaline pHs can be explained by additional Mo(0) oxidation/dissolution as MoO_4^{2-} molybdate anions at high pH, followed by precipitation on the surface as hydrated/hydroxylated MoO_3 oxides upon DI water rinsing at neutral pH. During the Mo(0) dissolution/oxidation process, most of the surface contaminants (particles, organic

residue) are removed by being dispersed in the cleaning formulation and the overall particle defectivity remains very low.

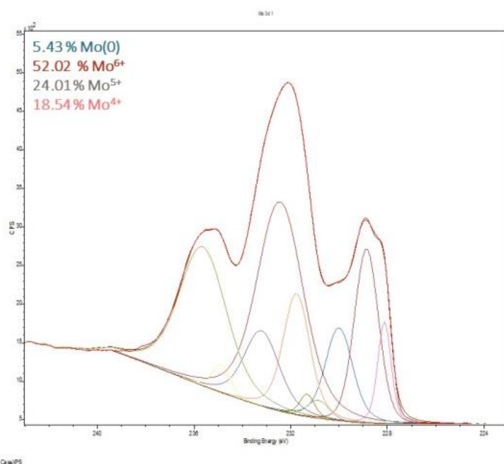

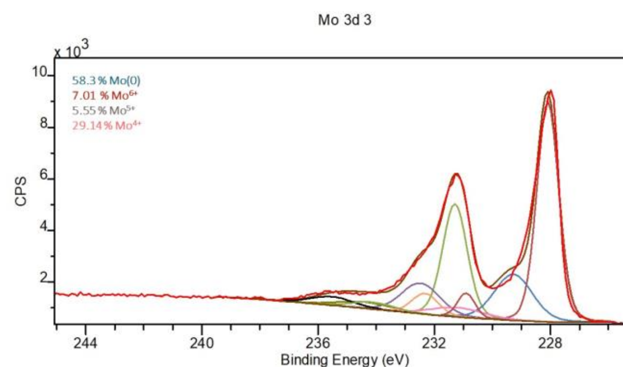

Figure 11 Mo 3d XPS spectrum post-CMP with TiO2 slurry

Figure 12 Mo 3d XPS spectrum post-CMP with SiO_2-based slurry

The effect of the type of abrasive particles used in the CMP slurry has a tremendous effect on the admixture of Mo oxides formed during the CMP step. Figures 11 and 12 represent Mo 3d XPS spectra of Mo ^{films} polished with low pH TiO_2-based slurry abrasive (Figure 11) vs. low pH SiO_2-based abrasive, Slurry C (Figure 12). TiO_2-based slurry generates a highly oxidized surface, mostly enriched in high oxidation state oxides, MoO_3 and Mo_2O_5 suboxides (> 76% of total oxides), while SiO_2-based slurry C generates a poorly oxidized surface, composed mostly of Mo(0), ~ 58% and Mo^{4+} (MoO_2), ~ 30%, leaving the highest oxidation states below 12%. This can be an additional confirmation that the superior oxidative strength of the TiO_2/H_2O_2 particle/oxidizer pair comes from both the high energy superoxide radicals generated at the TiO_2 nanoparticles surface and the direct oxidation of Mo(0) by the TiO_2 particles (evidence of increased reduced Ti^{3+} species in the slurry waste).

CONCLUSIONS

CMP and post-CMP cleaning performance of molybdenum and dielectric surfaces is highly dependent on the polishing slurry abrasive, slurry waste composition and interaction with the films, and the cleaning formulation pH, in addition to the slurry and cleaner organic additives, metal cations and other contaminants inherent to the environment. Low pH titania-based slurry abrasive in the presence of H_2O_2 as oxidizer leads to a more forceful Mo surface oxidation to an admixture of oxides with the Mo^{6+}/Mo^{5+} surface species. A composite, homogeneous material based mainly on titanium molybdate was identified by Raman and XPS spectroscopy in the slurry waste. Mo CMP with low pH silica-based slurry abrasives in the presence of H_2O_2 results in partially oxidized polished films, with the surface being dominated by Mo(0) and lower oxidation state Mo^{4+}(MoO_2) oxides. Analysis of the slurry waste precipitate indicated particle agglomeration based on > 90 % silica particles/organic additives composites, while the dried polishing waste supernatant was enriched in aqueous monomeric or oligomeric peroxomolybdates. Best cleaning performance/lowest particle defectivity on all three films (Mo, PETEOS and Si_3N_4) was achieved by CMP with silica-based Slurry C, followed by post-CMP cleaning in alkaline conditions.

REFERENCES

[1] V. Founta et al., Materialia 24 (2022), 101511
[2] M. R. Baklanov et al., ECS J. Solid State Sci. Technol. 4 (2014), Y1-Y4
[3] J. S. Clarke et al., 2014 IEEE Symp. VLSI Technol. (2014), 142-143
[4] S. Dutta et al., J. Appl. Physics 122 (2017), 025107
[5] H. Y. Ryu et al., ECS J. Solid State Sci. Technol. 10 (2021), 094001
[6] P. He et al., ECS J. Solid State Sci. Technol. 7(6) (2018), P299-P304
[7] D. White et al., Mater. Res. Soc. Symp. Proc. 1249 (2010), E04-04
[8] D. White et al., US Pat 8,008,202B, 2011
[9] J. A. Chudek et al., J. Chem. Soc. Faraday Trans. 90 (1994), 3699
[10] G. A. Nazri et al., Solid State Ionics 51-56 (1992), 376-382
[11] H. Uchiyama et al., Inorganic Chemistry 60 (6) (2021), 3593-3603
[12] M. S. Lee et al., Bulletin of The Korean Chemical Society 32 (2011), 3687-3691

ACKNOWLEDGEMENTS

The authors would like to thank Akshay Rajopadhye, Aaron Walsh, Rajiv Singh, Michael Owens, Michael Deangelo and Charlotte Chen. Permission given by Entegris to publish and present this work is gratefully acknowledged.

Corresponding Author:
Daniela White
Tel: +1 203-739-1470
E-mail: daniela.white@entegris.com
Entegris R&D SPI
7 Commerce Dr.
Danbury, CT 06810, USA